COBEM 2023 27TH INTERNATIONAL CONGRESS OF MECHANICAL ENGENEERING

ABCM Brazilian Society of Mechanical Sciences and Engineering
27th ABCM International Congress of Mechanical Engineering
December 04-08, 2023, Florianópolis-SC, Brazil

COB-2023-1246
NUMERICAL SIMULATION OF JET BUCKLING PHENOMENON OF VISCOELASTIC FLUID

Reginaldo Merejolli
Federal University of Grande Dourados, FACET-UFGD, Dourados-MS, Brazil
reginaldomerejolli@ufgd.edu.br

Caroline Viezel
Department of Mathematics and Computer Science, FCT-Unesp, P. Prudente-SP, Brazil
carol.viezel@gmail.com

Laís Corrêa
Federal University of Grande Dourados, FACET-UFGD, Dourados-MS, Brazil
laiscorrea@ufgd.edu.br

Gilcilene S. Paulo
Department of Mathematics and Computer Science, FCT-Unesp, P. Prudente-SP, Brazil
gilcilene.sanchez@unesp.br

This work presents a numerical method for simulating three-dimensional viscoelastic free surface flows with focus on the jet buckling phenomenon using the Giesekus constitutive equation. Industrial applications of fluid flow with free surfaces are always present: applications including casting, container filling, extrusion and fluid jetting devices. The precise determination of the free surface is important especially if the flow is even determined by the position and curvature of the free surface. Therefore, there is an industrial interest in developing numerical tools that are capable of dealing with these free surface flow problems in both two and three-dimensions. However, this is not an easy task, since, in addition to solving the governing equations, it is necessary to determine the free surface of the fluid, which varies with time and space. Another challenge is to simulate flows subject to high Weissenberg numbers, since most numerical methods become unstable for Weissenberg $>>1$. In order to overcome these challenges, the momentum equations are solved by a first order finite difference method on a staggered grid, while the Giesekus equations are tackled by a finite difference technique involving the conformation tensor, and the free surface is modelled by a front tracking technique based on the Marker-and-Cell method. The presented numerical method is verified by comparing the results obtained through mesh refinement for the flows in a tube and for a jet focusing on a flat plate (jet buckling). Convergence results were obtained by means of mesh refinement of the fully developed flow in a tube. Numerical results obtained from the simulation of the jet buckling include the measurements of the frequency of buckling for several values of the Weissenberg number. Additionally, the effect of the mobility parameter on the jet buckling phenomenon is investigated using high values of the Weissenberg number.

Keywords: *Giesekus Model, Jet Buckling, Viscoelastic Flow, Free Surface, Marker and Cell Method.*

1. INTRODUCTION

Many industrial manufacturing processes encounter challenges related to the fluid flows with free surfaces. These issues arise in various applications, including casting, container filling, extrusion, and fluid jetting devices. Accurately determining the behavior of the free surface becomes crucial when the flow is strongly influenced by its position and curvature. Moreover, these flows often are non-Newtonian and involves viscoelastic fluids flowing into containers with complex shapes. Therefore, there is a significant interest in the industrial sector to develop numerical tools capable of effectively addressing these problems in both two and three dimensions. Consequently, the numerical simulation of viscoelastic free surface flows has become a focal point of intense research (e.g. Tomé *et al.* (2010); Mompean *et al.* (2011); Tomé *et al.* (2014)). In the literature, a considerable amount of numerical solution of viscoelastic models can be found. For instance, differential models such as, Upper Convected Maxwell (UCM), Oldroyd-B, Phan-Thien-Tanner (PTT), and Giesekus models have been the subject of study of many researchers. Of these, the Giesekus model has been investigated by several researchers, e.g., Schleiniger and Weinacht (1991); Ferrás *et al.* (2012); Mu *et al.* (2013). However, when it comes to free surface flows, this particular model has received limited attention. In this study, our aim is to develop a numerical methodology for solving three-dimensional viscoelastic free surface flows using the Giesekus

constitutive equation. Subsequently, we will apply this methodology to simulate the jet buckling phenomenon. The structure of this work is as follows: Section 2 introduces the governing equations, along with the mathematical and numerical formulations. In Section 3, the convergence of the numerical method are assessed by mesh refinement obtained from simulations of a tube filling problem and a jet flow focusing on a flat plate. Section 4 presents the results obtained from the jet buckling phenomenon. Finally, the conclusions of this work are presented in Section 5.

2. MATHEMATICAL AND NUMERICAL FORMULATION

The governing equations for incompressible isothermal flows modelled by the Giesekus model (Schleiniger and Weinacht, 1991) are the mass and momentum equations together with the the Giesekus constitutive equation, that, in dimensionless form, can be written as:

$$\frac{\partial \mathbf{u}}{\partial t} + \nabla \left(\mathbf{u}\mathbf{u}^T\right) = -\nabla p + \frac{1}{Re}\nabla^2 \mathbf{u} + \nabla \cdot \mathbf{S} + \frac{1}{Fr^2}\mathbf{g}, \tag{1}$$

$$\nabla \cdot \mathbf{u} = 0, \tag{2}$$

$$\frac{\partial \tau}{\partial t} + \nabla \cdot (\mathbf{u}\tau) - (\nabla \mathbf{u}) \cdot \tau - \tau \cdot (\nabla \mathbf{u})^T + \tau + \alpha \frac{ReWi}{1-\beta}(\tau \cdot \tau) = 2\frac{1-\beta}{Re}\mathbf{D}. \tag{3}$$

The Elastic-Viscous-Splitting-Stress (EVSS) transformation (Rajagopalan *et al.*, 1990) was utilized to derive the transformed momentum equations, given by Eqs. (1) and (2). This transformation enables the representation of the extra-stress tensor as a linear combination of a Newtonian tensor and a non-Newtonian stress tensor, that models the elastic effects in the flow. The EVSS transformation is expressed as follows:

$$\tau = \frac{2}{Re}\mathbf{D} + \mathbf{S}, \tag{4}$$

which was already employed in the formulation of the momentum equations (1) and (2). In the Eqs. (1)-(4), t is the time, $\mathbf{u}$ is the velocity field, p is the pressure, $\mathbf{g}$ is the gravitational field, $\mathbf{S}$ is a non-Newtonian tensor, $\mathbf{D} = \frac{1}{2}\left((\nabla \mathbf{u}) + (\nabla \mathbf{u})^{\mathbf{T}}\right)$ is the Newtonian contribution to the extra-stress tensor and α is the parameter that models the mobility of the fluid. The nondimensional numbers, $Fr = \frac{U}{\sqrt{gL}}$, $Re = \frac{\rho UL}{\eta_0}$, $Wi = \frac{\lambda U}{L}$ are, respectively, the Froude, Reynolds and Weissenberg numbers. The constants L, U and ρ denote typical scalings for length, velocity and density, respectively. Furthermore, the amount of Newtonian solvent present in the fluid is controlled by the constant $\beta = \frac{\eta_s}{\eta_0}$, where $\eta_0 = \eta_s + \eta_p$ represents the total viscosity at zero shear, while η_s and η_p represent the Newtonian and polymeric viscosities, respectively. When $\alpha = 0$, the Giesekus model reduces to the Oldroyd-B model and making $\alpha = \beta = 0$, to the UCM model.

In order to solve the Eqs. (1)-(4), it is essential to define suitable initial and boundary conditions. At the inlet, the velocity is specified as $\mathbf{u} = \mathbf{U}_{inf}$, while the extra-stress tensor is set to $\tau = \tau_{inf}$. For fluid exits (outflows), homogeneous Neumann conditions are imposed for both velocity and extra-stress tensor, with $\frac{\partial \mathbf{u}}{\partial \mathbf{n}} = \frac{\partial \tau}{\partial \mathbf{n}} = \mathbf{0}$, $\mathbf{n}$ is the orthogonal direction on the exit boundary. On rigid boundaries, the no-slip condition, $\mathbf{u} = \mathbf{0}$, is assumed.

Our focus lies on three-dimensional flows with free surfaces in which the fluid flows enters a passive atmosphere. Under the assumption that surface tension forces can be disregarded at the interface between the fluids (viscous fluid and air), the extra-stress tensor components should be continuous. Consequently, the appropriate boundary condition is defined as follows (for details, see (Batchelor, 1967)):

$$\mathbf{n}^T \cdot (\sigma \cdot \mathbf{n}) = 0, \qquad \mathbf{m_1}^T \cdot (\sigma \cdot \mathbf{n}) = 0, \qquad \mathbf{m_2}^T \cdot (\sigma \cdot \mathbf{n}) = 0,$$

where $\mathbf{n}, \mathbf{m_1}$ and $\mathbf{m_2}$ denote unit normal and tangential vectors to the free surface and $\sigma = -p\mathbf{I} + \frac{2}{Re}\mathbf{D} + \mathbf{S}$ is the total stress tensor. These conditions are enforced by locally approximating the unit vectors $\mathbf{n}, \mathbf{m_1}$ and $\mathbf{m_2}$. Further details regarding the employed approximations can be found in Tomé *et al.* (2012).

The solution method employed in this study is based on the projection method initially introduced by Chorin and Marsden (2000). Building upon this foundation, the present methodology is grounded in the GENSMAC (GENeralized Simplified Marker-And-Cell) approach, which has in constant improvement by Tomé and McKee (1994) and co-workers Tomé *et al.* (2012).

In this methodology, the momentum equations are solved on a 3D-staggered grid. The Giesekus constitutive equation, on the other hand, is solved by a finite difference method that approximates the time derivative with a second-order Runge-Kutta method. The spatial derivatives are approximated using second-order differences. Further insights into the cell classification and the discretization of the equations at the free surface can be found in the work of McKee *et al.* (2008).

3. VERIFICATION RESULTS

In order to verify the capability of the numerical methodology presented in Section 2, two different simulations were performed to analyze the mesh refinement: the filling of a three-dimensional tube and the jet flow onto a rigid plate.

3.1 3D-tube filling

A simulation of the filling of a three-dimensional tube was conducted to analyse the convergence of the numerical results. For this, the problem was solved using five different computational meshes: M1: $16 \times 16 \times 80$ cells ($dx = dy = dz = 0.125$), M2: $20 \times 20 \times 100$ cells ($dx = dy = dz = 0.1$), M3: $32 \times 32 \times 160$ cells ($dx = dy = dz = 0.0625$), M4: $40 \times 40 \times 200$ cells ($dx = dy = dz = 0.05$) and Mref: $80 \times 80 \times 400$ cells ($dx = dy = dz = 0.025$).

The filling process consisted of considering a totally empty tube at time $t = 0s$. Subsequently, the fluid is injected through the tube entrance until it reached a state of complete fullness and steady state flow was established. For the simulations, the following data were considered: tube radius $L = 1m$, tube length $10L$, $U = 1m/s$, $Re = 1.0$, $Wi = 1.0$, $\beta = 0.5$ and $\alpha = 0.1$.

Figure 1(a) shows the frontal visualization of the filling of a three-dimensional tube at the time $t = 5s$, while Figs. 1(b)-1(e) display the numerical profiles obtained for velocity w and extra-stress tensor components τ^{xx}, τ^{xz} and τ^{zz} at the middle section of the tube ($z = 5, y = 1$ and $0 < x < 2$), respectively. From Fig. 1, we can observe that the numerical solutions displayed satisfactory agreement with the solution obtained on the finer mesh (Mref), which indicates convergence of the results.

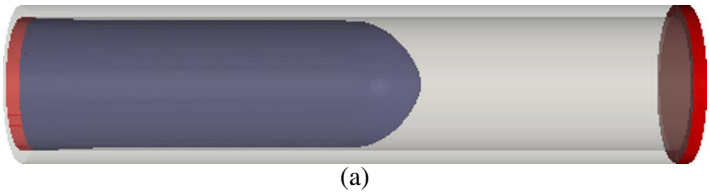

(a)

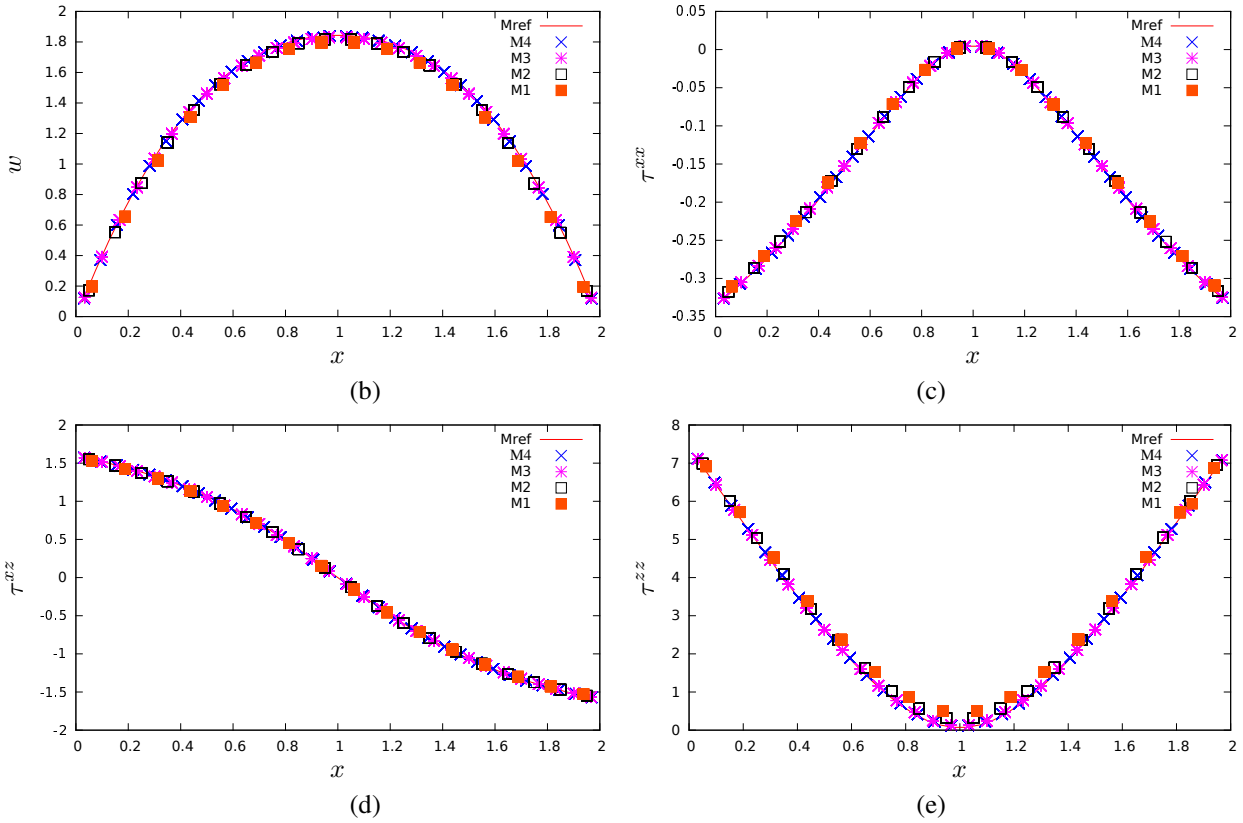

Figure 1. Filling of a tube with a viscoelastic fluid: $Re = 1$, $Wi = 1$, $\beta = 0.5$ and $\alpha = 0.1$. (a) Three-dimensional visualization of the flow at $t = 5s$. Figures (b)-(e) display the solutions at the middle of the tube at $t = 50s$: (b) w, (c) τ^{xx} , (d) τ^{xz} (e)τ^{zz}.

The convergence of the numerical method was also verified quantitatively by comparing the results obtained from the meshes M1, M2, M3, and M4 with the reference mesh, Mref. Table 1 presents the obtained relative errors for the different meshes simulations. It can be observed that as the mesh is refined, the relative error decreases, demonstrating the convergence of the presented numerical method.

Table 1. The relative errors in the M1, M2, M3 and M4 meshes, compared to the Mref mesh, for the filling of a three-dimensional tube problem.

Malhas	$E(w)$	$E(\tau^{xz})$	$E(\tau^{xx})$	$E(\tau^{zz})$
M1	3.65×10^{-2}	1.43×10^{-2}	2.97×10^{-2}	7.18×10^{-2}
M2	2.03×10^{-2}	8.08×10^{-3}	1.67×10^{-2}	4.15×10^{-2}
M3	7.68×10^{-3}	4.27×10^{-3}	7.51×10^{-3}	8.36×10^{-3}
M4	3.66×10^{-3}	1.55×10^{-3}	3.14×10^{-3}	7.82×10^{-3}

3.2 Jet flow onto a rigid plate

To validate the proposed numerical methodology in Section 2, a mesh refinement study was also conducted for the phenomenon of the jet flow onto a rigid plate. The data employed in these simulations were as follows: injector diameter $D = 1$, height of the injector above the rigid plate $H = 15$, injection velocity $U = 1.0$, Froude number $Fr = 2.5240$, Reynolds number $Re = 1.5$, Weissenberg number $Wi = 10$ and $\alpha = 0.01$. Four computational meshes were employed: $M_1 : h = D/8 = 0.125$, $(48 \times 48 \times 136$ cells$)$; $M_2 : h = D/10 = 0.10$, $(60 \times 60 \times 170$ cells$)$; $M_3 : h = D/12 = 0.083333$, $(72 \times 72 \times 204$ cells$)$ e $M_4 : h = D/14 = 0.071428$, $(84 \times 84 \times 238$ cells$)$.

Figure 2 presents the visualization of the jet surface obtained from the simulations conducted using the four different meshes. It can be observed that there is good agreement among the results, confirming mesh independence in solving this problem.

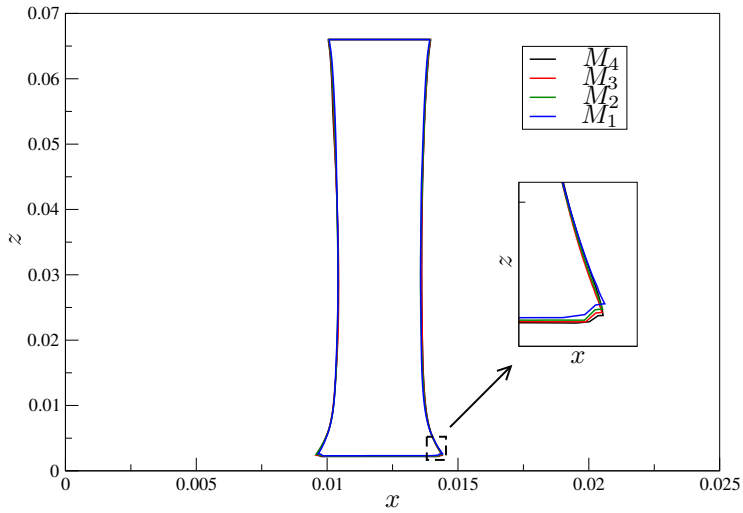

Figure 2. Jet flow onto a rigid plate reaching the bottom of the box using multiple meshes. Visualization obtained in the xz plane.

4. JET BUCKLING PHENOMENON

The numerical methodology proposed in Section 2, which was verified in Section 3, is now applied to simulate three-dimensional viscoelastic free surface flows, specifically the jet buckling phenomenon.

When a viscous jet impinges upon a rigid plate, several phenomena can occur, one of which is jet buckling. This phenomenon is typically observed in highly viscous jets and has attracted significant attention from many researchers in recent decades (e.g. Paulo *et al.* (2007), Ville *et al.* (2011), Tomé *et al.* (2012), Cruickshank and Munson (1981) and Cruickshank (1988)).

It is well known that, for a Newtonian fluid, the Reynolds number is an important parameter that controls the buckling phenomenon. On the other hand, in viscoelastic flows, the Weissenberg number models the elastic forces in the flow and also has a strong influence on the buckling phenomenon, as it was demonstrated in the works Paulo *et al.* (2007) and Tomé *et al.* (2012).

To highlight the effect of the Weissenberg number on the jet buckling phenomenon, the Fig. 3 depicts the results obtained with $Re = 1.5$, $\alpha = 0.01$ and different values of the Weissenberg number at times $t = 125$ and 250. It can be observed from this figure that, for $Wi = 10$ and $Wi = 50$, the buckling effect occurs, with its presence being more pronounced for $Wi = 10$. However, an increase in the Weissenberg number resulted in fluid agglomeration in the center of the box. It is believed that these effects are caused by the increased fluid elasticity (Tomé *et al.*, 2012).

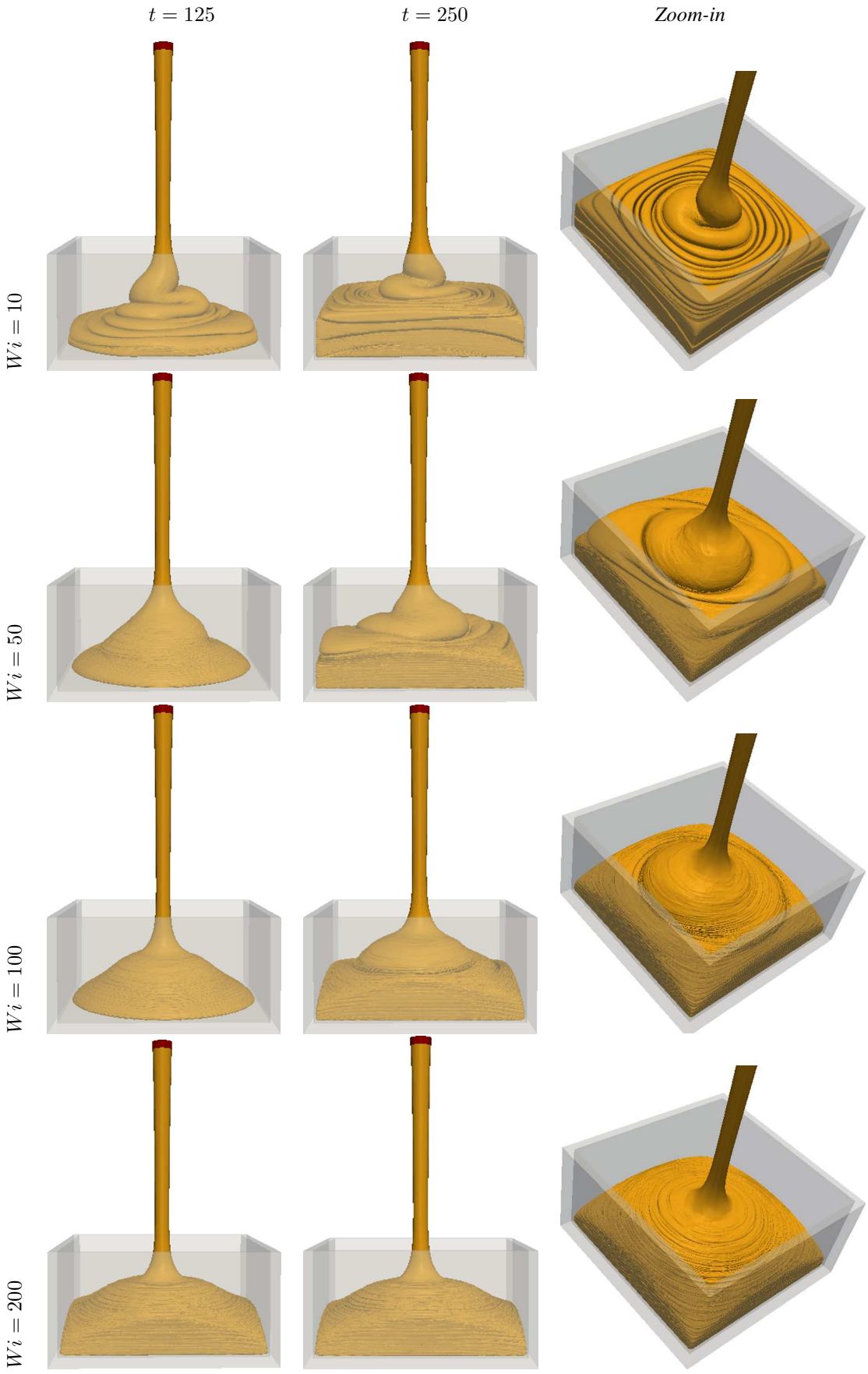

Figure 3. Jet buckling simulation at times $t = 125$ and $t = 250$, $Re = 1.5$, $\alpha = 0.01$ and for different values of Wi.

5. CONCLUDING REMARKS

This paper presented a finite difference technique to simulate viscoelastic flows governed by the constitutive equation Giesekus. Verification results in the problems of filling a circular tube and a jet flow onto a rigid plate were provided, where mesh refinement showed convergence of the numerical methodology. The technique was applied to simulate the jet buckling phenomenon for various values of the Weissenberg number. The numerical results showed that, for $Wi = 10$ and $Wi = 50$, the buckling effect occurs (being more pronounced for $Wi = 10$). Nevertheless, as the Weissenberg number increased, fluid agglomeration in the center of the box occurred. These effects are attributed to the heightened fluid elasticity.

6. ACKNOWLEDGEMENTS

This work is a tribute and posthumous gratitude for Prof Dr Murilo F. Tomé who sowed curiosity and passion for the behavior of complex flows, mainly involving free surface and viscoelastic fluids. He dedicated his life with great enthusiasm to the academy and to his advisees, offering opportunities to participate in his projects and his great friendship.

7. REFERENCES

Batchelor, G.K., 1967. *An Introduction to Fluid Dynamics*. Cambridge University Press.

Chorin, A.J. and Marsden, J.E., 2000. *A Mathematical Introduction to Fluid Mechanics*. Springer.

Cruickshank, J.O., 1988. "Low - Reynolds - number instabilities in stagnating jet flows". *Journal of Fluid Mechanics*, Vol. 113, pp. 111–127.

Cruickshank, J.O. and Munson, B.R., 1981. "Viscous-fluid buckling of plane axisymmetric jets". *Journal of Fluid Mechanics*, Vol. 113, pp. 221–239.

Ferrás, L.L., Nóbrega, J.M. and Pinho, F.T., 2012. "Analytical solutions for channel flows of Phan - Thien - Tanner and Giesekus fluids under slip". *Journal of Non-Newtonian Fluid Mechanics*, Vol. 171-172, pp. 97–105.

McKee, S., Tomé, M.F., Ferreira, V., Castelo, A., Sousa, F. and Mangiavacchi, N., 2008. "The MAC method". *Computers & Fluids*, Vol. 37, pp. 907–930.

Mompean, G., Thais, L., Tomé, M.F. and A., C., 2011. "Numerical prediction of three-dimensional time-dependent viscoelastic extrudate swell using differential and algebraic models". *Computers & Fluids*, Vol. 44, pp. 68–78.

Mu, Y., Zhao, G., Chen, A. and Wu, X., 2013. "Modeling and simulation of tree-dimensional extrusion swelling of viscoelastic fluids with PTT, Giesekus and FENE-P constitutive models." *International Journal for Numerical Methods in Fluids*, Vol. 72.

Paulo, G.S., Tomé, M.F. and McKee, S., 2007. "A marker-and-cell approach to viscoelastic free surface flows using the PTT model". *Journal of Non-Newtonian Fluid Mechanics*, Vol. 147, pp. 149–174.

Rajagopalan, D., Armstrong, R.C. and Brown, R.A., 1990. "Finite element methods for calculation of steady, viscoelastic flow using constitutive equations with a newtonian viscosity". *Journal of Non-Newtonian Fluid Mechanics*, Vol. 36, pp. 159–192.

Schleiniger, G. and Weinacht, R.J., 1991. "Steady Poiseuille flows for a Giesekus fluid". *Journal of Non-Newtonian Fluid Mechanics*, Vol. 40, pp. 79–102.

Tomé, M.F., Castelo, A., Afonso, A., Alves, M.A. and Pinho, F., 2012. "Application of the log-conformation tensor to three-dimensional time-dependent free surface flows". *Journal of Non-Newtonian Fluid Mechanics*, Vol. 175-176, pp. 44–54.

Tomé, M.F., Castelo, A., Nóbrega, J., Carneiro, O.S., Paulo, G.S. and Pereira, F.T., 2014. "Numerical and experimental investigations of three-dimensional container filling with newtonian viscous fluids". *Computers & Fluids*, Vol. 90, pp. 172–185.

Tomé, M.F. and McKee, S., 1994. "Gensmac: a computational marker-and-cell method for free surface flows in general domains". *Journal of Computational Physics*, Vol. 110, pp. 171–186.

Tomé, M.F., Paulo, G.S., Pinho, F. and Alves, M.A., 2010. "Numerical solution of the ptt constitutive equation for unsteady three-dimensional free surface flows". *Journal of Non-Newtonian Fluid Mechanics*, Vol. 165, pp. 247–262.

Ville, L., Silva, L. and Coupez, T., 2011. "Convected level set method for the numerical simulation of fluid buckling". *International Journal for Numerical Methods in Fluids*, Vol. 66, pp. 324–344.

8. RESPONSIBILITY NOTICE

The authors are solely responsible for the printed material included in this paper.